of gyration has also been found to increase with time. However, for the same TEOS/PTMO ceramers reacted in THF/IPA, the inorganic particles display more mass fractal behavior. The radius of gyration of the scattering particles also increases with time though the final particle size is much smaller than those developed in the DMF/IPA ceramers.

Acknowledgment. The authors would like to acknowledge the Office of Naval Research for their financial support as well as Don K. Brandom for his assistance with the computational treatement of the SAXS data.

Registry No. TEOS, 78-10-4; $Ti(OPr\text{-}i)_4$, 546-68-9; $Zr(OPr)_4$, 23519-77-9; polytetramethyleneglycol, isocyanatopropyltriethoxysilyl diester, 144126-55-6.

Novel Antimony Sulfides: Synthesis and X-ray Structural Characterization of $Sb_3S_5 \cdot N(C_3H_7)_4$ and $Sb_4S_7 \cdot N_2C_4H_8$

John B. Parise* and Younghee Ko

Department of Earth and Space Sciences, State University of New York, Stony Brook, New York 11794-2100

Received July 28, 1992. Revised Manuscript Received September 27, 1992

Novel antimony sulfides have been synthesized using hydrothermal techniques and organic amines as structure directing agents. The structures of two of these have been solved using single-crystal X-ray diffraction data. One, $Sb_3S_5 \cdot N(C_3H_7)_4$ (SbStpa), forms light yellow blades, has a second harmonic signal 4 times that of quartz, and was synthesized in the presence of tetrapropylammonium hydroxide. The structure contains independent chains of antimony sulfide, infinite in the [100] direction, which are separated by $[N(C_3H_7)]_4^+$ ions. These chains are comprised of edge-linked five-membered rings of SbS_3-pyramids. A second compound, $Sb_4S_7 \cdot N_2C_4H_8$ (SbSpip), crystallizes as red tablets in the presence of triethylenetetramine. The structure incorporates a breakdown product of the added amine, molecules of diprotonated piperazine, $[N_2C_4H_8]^{2+}$. The organic is accommodated between slabs of $[Sb_4S_7]^{2-}$, infinite in the (010) plane. These slabs consist of chains containing three-membered rings of SbS_3-pyramids joined by individual three-coordinated antimony sulfide moieties. Both structures crystallize in the space group *Ama*2 with $a = 10.360$ (2), $b = 23.474$ (3), $c = 9.336$ (1) Å for SbStpa and $a = 9.9498$ (9), $b = 28.513$ (4), and $c = 5.9032$ (8) Å for SbSpip.

Introduction

Recently there has been a growth of interest in novel sulfide structure types.[1-5] This curiosity is sparked by the perceived need to engineer new materials with useful electrical, optical, and ion-exchange properties, or to obtain substances which may be helpful as precursors in the synthesis of such materials.[4] One of the more successful strategies in the *directed* synthesis of oxide materials has recently been applied to sulfides.[1-3] The technique[6] involves the introduction of organic amines into oxide gels or sulfide slurries, followed by hydrothermal crystallization. In the case of oxides, open framework or 2-D structures related to the aluminosilicate zeolites and molecular sieves result.

Using hydrothermal techniques[6-16] adapted for the synthesis of molecular sieves, new open framework materials have been produced from Sb_2S_3.[2,3] In this work, the finely divided sulfide was treated hydrothermally in the presence of alkali metals,[2,6-13] alkali-earth metals,[14] or tertiary amines.[1,3,15,16] These occluded the channels formed about them and were thought to act as structure directing or "templating" agents, during crystallization.[17-19] Further, the black powders recrystallized to produce materials, red[2] to orange[3] in color; this change in color correlated with a decrease in density of the antimony sulfide framework, suggesting an increase in the bandgap.

A natural extension of this work is the use of larger tertiary amines in an attempt to further vary the optical properties and possibly produce materials with larger cavities or with lower structural dimensionality. Reported in this paper are the syntheses of new materials, produced according to this strategy, along with the crystal structures of two of these.

Experimental Section

Synthesis and Characterization. A variety of organic amines (Aldrich Chemical, Table I) have been used in an attempt to direct recrystallization of Sb_2S_3 (Aldrich Chemical). Each potential template was mixed with Sb_2S_3 and H_2O and, in some cases, the amine was reacted with H_2S prior to introduction to the slurries. Addition of H_2S was sometimes found to be efficacious in the

(1) Bedard, R. L.; Wilson, S. T.; Vail, L. D.; Bennett, J. M.; Flanigen, E. M. In *Zeolites: Facts, Figures, Future*; Jacobs, P. A., van Santen, R. A. Eds.; Elsevier Publishing: Amsterdam, 1989.
(2) Parise, J. B. *J. Chem Soc., Chem. Commun.* **1990**, 1553.
(3) Parise, J. B. *Science* **1991**, *251*, 293.
(4) Kanatzidis, M. G. *Comments Inorg. Chem.* **1990**, *10*, 161.
(5) Krebs, B. *Angew. Chem., Int. Ed. Engl.* **1983**, *22*, 113.
(6) Graf, H. A.; Schäfer, H. *Z. Naturforsch.* **1972**, *27b*, 735.
(7) Volf, K.; Schäfer, H. *Z. Naturforsch.* **1978**, *33b*, 827.
(8) Volf, K.; Schäfer, H. *Z. Naturforsch.* **1979**, *34b*, 172.
(9) Eisenmann, B.; Schäfer, H. *Z. Naturforsch.* **1979**, *34b*, 383.
(10) Volf, K.; Schäfer, H. *Z. Naturforsch.* **1979**, *34b*, 1637.
(11) Graf, H. A.; Schäfer, H. *Z. Anorg. Allg. Chem.* **1975**, *414*, 211.
(12) Dittmar, G.; Schäfer, H. *Z. Anorg. Allg. Chem.* **1978**, *441*, 93.
(13) Dittmar, G.; Schäfer, H. *Z. Anorg. Allg. Chem.* **1978**, *441*, 98.
(14) Cordier, G.; Schäfer, H.; Schwidetzky, C. *Z. Naturforsch.* **1984**, *39b*, 131.
(15) Volf, K.; Bickert, P.; Kolmer, R.; Schäfer, H. *Z. Naturforsch.* **1979**, *34b*, 380.
(16) Dittmar, G.; Schäfer, H. *Z. Anorg. Allg. Chem.* **1977**, *437*, 183.
(17) Barrer, R. M. *Hydrothermal Chemistry of the Zeolites*; Academic Press: London, 1982.
(18) Wilson, S. T.; Lok, B. M.; Flanigen, E. M. U.S. Patent 4,310,440, 1982.
(19) Parise, J. B. *J. Chem Soc., Chem. Commun.* **1985**, 606.

0897-4756/92/2804-1446$03.00/0

Table I. Typical Synthetic Conditions for Novel Antimony Sulfide Materials.

struct type	amine	color	slurry composition (mol) Sb_2S_3	H_2S	amine	H_2O	temp (°C)	time (h)
1	TEA[a]	yellow	1	0	1–3	15–30	150	24
2	TPA[b]	yellow	1	0	1–3	15–30	70–150	24–48
3	TBA[c]	yellow	1	0	1	30	100	48
4	DABCO[d]	red	1	0.3–1	1	30	200	24
5	TETN[e]	dark red	1	0.3–1	1	30	200	72
5	EN[f]	dark red	1	0.3–1	1	30	200	72
6	TETN	bright red	1	0.3–1	1	30	200	24
4	TETN	red	1	0.3–1	1	30	200	168
7	pyrrolidine	dark red	1	0.3	1	30	200	24
4	piperazine	red	1	0.3	1	30	200	24

[a] Tetraethylammonium hydroxide. [b] Tetrapropylammonium hydroxide. [c] Tetrabutylammonium hydroxide. [d] Triethylenediamine. [e] Triethylenetetramine. [f] Ethylenediamine.

Table II. X-ray Diffraction Data for Novel Antimony Sulfides

struct type	amine[a]	*d* spacings of strongest XRD lines (Å)						
1	TEA[b]	9.700	4.785	10.825	5.513	13.684	7.809	5.286
2	TPA[c]	8.679	11.635	2.979	4.659	7.723	4.345	5.833
3	TBA	14.033	8.763	11.139	15.443	9.235	5.993	7.692
4	DABCO, piperazine, TETN[c]	14.565	7.174	4.115	4.296	5.023	5.791	4.754
5	EN[d], TETN	11.513	5.654	4.019	12.701	7.310	3.909	3.154
6	TETN	17.453	8.813	10.825	5.846	14.033	4.398	4.072
7	pyrrolidine	17.459	8.838	13.599	6.736	3.347	3.914	2.993

[a] See Table I for definition of amines used. [b] Subcell for SbStea: a = 14.46, b = 26.43, c = 18.68 Å. [c] Batches from which crystals were chosen for structural analysis. [d] Subcell for SbSen: a = 11.30, b = 22.81, c = 10.03 Å.

production of unique materials or to aid in crystal growth. The pH of the reaction mixtures to which H_2S was added, was between 7 and 10; the remainder had pH values greater than 10. The starting amounts of Sb_2S_3 were always 1.3 mmol with the remaining ingradients in the ratios given in Table I. Sb_2S_3 was mixed first with H_2O, then organic amines were added at room temperature. The resultant slurries were divided between two or three Pyrex tubes and were heated at temperatures between 50 and 200 °C for 1–7 days in stainless hydrothermal bombs (Table I). The products were isolated by filtration, washed with deionized water and ethanol, and dried at room temperature. The yields of these reactions were greater than 80% (based on Sb_2S_3).

Each structure type displays a characteristic X-ray powder diffraction (XRD) pattern, the more intense lines of which are given in Table II. Comparison of the XRD patterns with those of known phases suggested that the materials were novel. Seven structure types have thus far been isolated in pure form. Of these, triethylenetetramine (TETN) directs the formation of three. The TETN molecule is known to decompose to ethylenediamine and cyclized amines, including piperazine,[20] under conditions similar to those used in the syntheses summarized in Table I.

With the exception of structure types 3 and 7 (Table I), the materials formed a single crystals up to 300 μm on edge. In common with others in this series,[2,3] single-crystal diffraction photographs of some of the compounds displayed patterns of commensurate or incommensurate satellite reflections based upon simpler subcells (Table II). The crystals chosen for data analysis were from batches containing TETN and tetrapropylammonium (TPA) hydroxide in the unreacted slurries. They were not afflicted with overly complex diffraction patterns. Qualitative chemical analysis, using a microprobe X-ray analyzer, confirmed the presence of nitrogen, as was to be expected for a growth mechanism that included the templates employed here. There was no evidence for partial substitution of sulfide by oxygen. Quantitative microprobe analysis of the TPA material indicated Sb, S, and N were in the ratio 3:5:1; this result was subsequently confirmed by the analysis of single-crystal X-ray diffraction data.

Thermogravimetric analysis of several of the materials described in Tables I and II showed that changes in weight occurred between 200 and 300 °C. The X-ray powder diffractions of materials recovered following these experiments matched that for Sb_2S_3, indicating the collapse of the sulfide frameworks.

Table III. Summary of X-ray Diffraction Data for SbStpa and SbSpip

formula (asym unit)	$Sb_3S_5{\cdot}N(C_3H_7)_4$	$Sb_4S_7{\cdot}N_2C_4H_8$
color, shape	yellow, terminated prism	red, tablets
space group	*Ama*2	
a, Å	10.360 (2)	9.9498 (9)
b, Å	23.474 (3)	28.513 (4)
c, Å	9.336 (1)	5.9032 (8)
temp, °C	22	
vol, Å^3	2270.4	1674.7
Z	4	
formula wt	711.9	975.6
calcd density, g/cm^3	2.083	3.155
μ(Mo), cm^{-1}	40.1	72.6
diffractometer	Enraf-Nonius CAD-4	Huber
radiation	Mo Kα	
data collected	6093	2868
merge R	0.021	
min and max 2θ, deg	2–60	2–62
max $\lvert h\rvert$, $\lvert k\rvert$, $\lvert l\rvert$	13, 32, 14	14, 40, 8
data octants	+++, ++−, +−+, −++	+++, ++−
scan method	ω	$\omega/2\theta$
abs method	analytical	
no. of unique data ($I > \beta\sigma(I)$)	3043 (*hkl* and *hk-l*)	2813
Refinement Method	full matrix least-squares on F	
anomalous dispersion	Sb and S	
weighting scheme	$\mu[\sigma^2(I) + 0.0008I^2]^{-1/2}$	
atoms refined	anisotropic: Sb,S,N,C; H atoms not included in calculation	
params varied	120	88
param/data ratio	25.36	31.97
R (second setting)	0.026 (0.028)	0.041 (0.044)
R_2 (second setting)	0.026 (0.029)	0.039 (0.042)
error of fit (second setting)	0.94 (1.04)	0.99 (1.06)

Structure Determination. *SbStpa*: Preliminary precession and Weissenberg photographs suggested an orthorhombic cell with extinction symbol *A–a–*. A positive test for nonlinear optical behavior[21] narrowed to choice of possible space groups to *Ama*2

(20) Hutchinson, W. M.; Collett, A. R.; Lazzell, C. L. *J. Am. Chem. Soc.* **1945**, *67*, 1966.

Table IV. Fractional Coordinates (×10⁴) and Isotropic Thermal Parameters for SbStpa

atom	site/occ	x	y	z	B_{iso}[a]
Sb(1)	8c/1.0	5694.6 (2)	9292.0 (1)	8570.7 (0)	2.8 (1)
Sb(2)	4b/1.0	2500	9213.0 (2)	9976.2 (5)	2.8 (1)
S(1)	4a/1.0	5000	10000	10354 (1)	2.7 (1)
S(2)	4b/1.0	7500	8924 (1)	9966 (2)	3.5 (1)
S(3)	4b/1.0	2500	9683 (1)	7714 (2)	3.3 (1)
S(4)	8c/1.0	4287.9 (9)	8525.3 (4)	9537 (2)	3.7 (1)
N(1)	4b/1.0	2500	8276 (3)	4468 (7)	5.6 (2)
C(1)	4b/1.0	2500	7970 (5)	5802 (11)	9.6 (5)
C(2)	8c/0.5	3027 (12)	7885 (5)	3259 (10)	5.5 (3)
C(3)	8c/1.0	3676 (18)	8640 (5)	4505 (18)	17.3 (7)
C(4)	4b/1.0	2500	7215 (4)	7613 (11)	8.4 (4)
C(5)	4b/1.0	2500	7099 (5)	1597 (12)	11.6 (6)
C(6)	8c/1.0	5547 (10)	9232 (4)	4079 (10)	8.6 (3)
C(7)	8c/1.0	4249 (16)	9017 (7)	3918 (21)	16.3 (7)
C(8)	8c/0.5	3221 (16)	7560 (5)	6331 (15)	7.6 (5)
C(9)	8c/0.5	2978 (14)	7477 (5)	2767 (15)	7.2 (5)

[a] Equivalent isotropic thermal parameter.

Table V. Fractional Coordinates (×10⁴) and Isotropic Thermal Parameters for SbSpip

atom	site/occ	x	y	z	B_{iso}[a]
Sb(1)	4b/1.0	7500	6275.0 (2)	5531.0 (0)	1.7 (1)
Sb(2)	8b/1.0	4553.2 (4)	5648.9 (1)	8359 (1)	1.4 (1)
Sb(3)	4b/1.0	2500	5057.5 (2)	2874 (1)	1.9 (1)
S(1)	4b/1.0	2500	6140 (1)	7924 (4)	1.6 (1)
S(2)	4b/1.0	7500	7062 (1)	4280 (5)	2.2 (1)
S(3)	8b/1.0	5699 (2)	6412 (1)	8289 (4)	2.4 (1)
S(4)	8b/1.0	4398 (2)	5632 (1)	2511 (3)	1.8 (1)
S(5)	4b/1.0	2500	4818 (1)	9027 (4)	1.9 (1)
N(1)	4b/1.0	2500	7575 (3)	4316 (15)	1.9 (2)
N(2)	4b/1.0	2500	6603 (3)	2920 (14)	1.9 (2)
C(1)	8b/1.0	3751 (7)	6901 (2)	2780 (15)	2.4 (2)
C(2)	8b/1.0	3732 (7)	7280 (2)	4564 (13)	2.1 (2)

[a] Equivalent isotropic thermal parameter.

or $A2_1am$. Subsequent structure analysis confirmed $Ama2$ as the correct space group symmetry for this material. Data were collected on an Enraf-Nonius CAD-4 diffractometer using the experimental parameters given in Table III. The cell parameters, also reported in Table III, were determined from 25 reflections with $6° < \theta < 23°$. Loretz, polarization and absorption corrections were applied.

The structure was determined from a starting model obtained by an automated Patterson interpretation procedure.[22] Successive cycles of least-squares refinement and the calculation of Fourier difference maps lead to the final model, summarized in Table IV. In this model two arms of the TPA molecule are disordered about the mirror perpendicular to the a axis (Table IV and Figure 1a), in a fashion similar to that observed in a recent accurate study of the aluminosilicate molecular sieve, ZSM-5[23]. The hydrogen atoms were not located, nor were their calculated positions included in determinations of the structure factors.

SbSpip: Preliminary investigations and the subsequent structure determination suggested this material also crystallized in the space group $Ama2$. Data were collected on a Huber diffractometer using the experimental parameters given in Table III. The cell parameters were determined from 15 reflections with $13° < \theta < 17°$. Data were corrected for Lorentz, polarization, and absorption effects.

The structure was solved using a combination of automated Patterson solution and Fourier difference techniques.[22] The geometry of the amine, a ring rather than the chain expected for the template molecule TETN, was located between slabs of antimony sulfide in the structure (Figure 1b). A series of refinements confirmed that the N or C sites in this six-membered ring (Table V) were fully occupied. Partial occupancy could result from the disorder of ethylenediamine about the mirror plane perpendicular to the a axis, on which the ring is located (Figure 1b, Table V). Ethylenediamine is a known product of the breakdown of TETN under the conditions used for the synthesis of SbSpip.[20] Additional refinements suggested that organic material was diprotonated piperazine, $[N_2C_4H_8]^{2+}$, with the two nitrogen atoms situated on the mirror plane (Table V). Refinements in which the N atoms were placed at other positions in the ring gave results inferior to those reported in Table III. To confirm the presence of piperazine, a sample of SbSpip was heated to 200 °C, and the volatiles were collected. An NMR spectrum corresponding to that expected for the piperazine molecule was obtained. The rearrangement of TETN under high-temperature conditions, to produce ethylenediamine and piperazine, is well documented.[20]

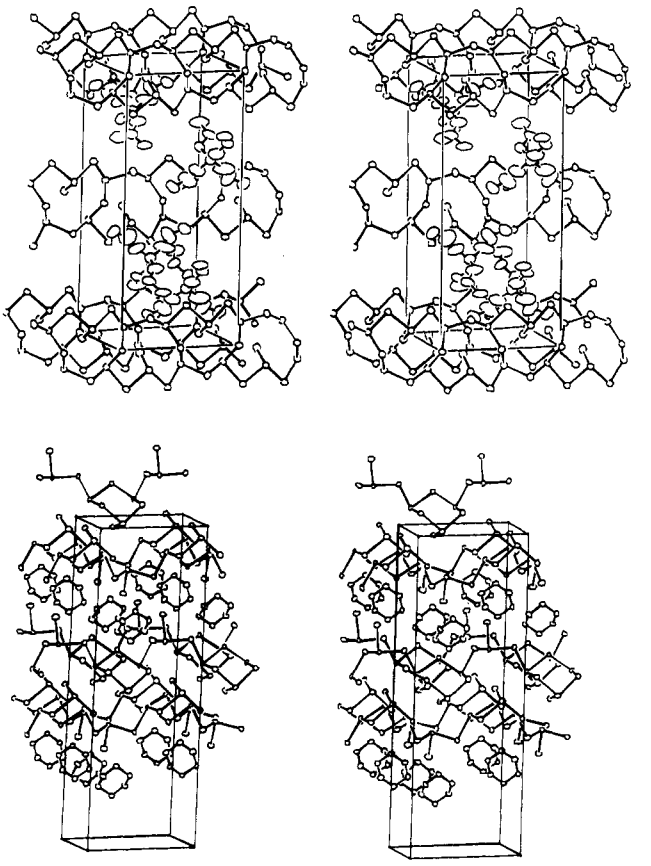

Figure 1. Stereo ORTEP drawing[24] of the structure of (a, top) $Sb_3S_5{\cdot}N(C_3H_7)_4$ and (b, bottom) $Sb_4S_7{\cdot}N_2C_4H_8$. The origins of the unit cells are in the back bottom left hand corner, with x to the right and y close to vertical. For the sake of clarity, only one orientation of the TPA molecule is shown in (a); it is disordered about the mirror planes perpendicular to the x direction. Only those Sb–S bonds < 2.5 Å are shown (see Figure 2).

Results and Discussion

Selected bond lengths and angles for SbStpa and SbSpip are given in Tables VI and VII. The structures of both compounds (Figure 1) have much in common with the other "templated" antimony sulfides described thus far.[2,3,6-16] As with $Sb_3S_5{\cdot}N(CH_3)_4$[3] (SbStma) and $Cs_6Sb_{10}S_{18}$,[2] the antimony sulfide forms a backbone of essentially three-coordinated Sb. The local geometries of the building units, which constitute SbSpip and SbStpa, are shown in Figure 2 and should be compared to similar diagrams in refs 2–16. Antimony is in approximately pyramidal coordination with sulfur, with three Sb–S distances less than 2.7 Å (Tables VI and VII). Some of the coordination spheres contain additional sulfurs at distances between 2.7 and 3.3 Å (Figure 2 and Tables VI and VII). However, unlike SbStma,[3] the compounds incorporating

(21) Kurtz, S. K.; Perry, T. T. *J. Appl. Phys.* **1968**, *39*, 3798.
(22) Calabrese, J. C., personal communication.
(23) Van Koningsveld, H.; Van Bekkum, H.; Jansen, J. C. *Acta Crystallog.* **1987**, *B32*, 127.
(24) Johnson, C. K. ORTEP Report ORNL-3794; Oak Ridge National Laboratory: Oak Ridge, TN, 1965.

Table VI. Selected Interatomic Distances (angstroms) and Angles (degrees) for SbStpa

Sb(1)–S(1)	2.4597 (9)	C(1)–C(8)	1.315 (15)
Sb(1)–S(2)	2.437 (1)	C(2)–C(2)^c	1.091 (24)
Sb(1)–S(4)	2.485 (1)	C(2)–C(9)^c	1.487 (16)
Sb(1)–S(3)^a	3.152 (1)	C(2)–C(9)	1.064 (17)
Sb(2)–S(1)	3.2007 (5)	C(3)–C(7)	1.196 (18)
Sb(2)–S(3)	2.382 (2)	C(4)–C(8)	1.626 (17)
Sb(2)–S(4)	2.491 (1)	C(5)–C(9)	1.492 (18)
N(1)–C(1)	1.437 (12)	C(6)–C(7)	1.446 (17)
N(1)–C(2)	1.553 (12)	C(8)–C(8)^c	1.492 (34)
N(1)–C(3)	1.489 (16)	C(9)–C(9)^c	0.990 (30)
S(1)···S(3)	3.652 (1)	C(8)···C(9)^c	3.556 (19)
S(2)···S(3)^a	3.888 (2)	C(8)···C(9)	3.342 (19)
S(1)–Sb(1)–S(2)	95.85 (5)	C(1)–N(1)–C(2)	109.5 (7)
S(1)–Sb(1)–S(4)	94.14 (3)	C(1)–N(1)–C(3)	105.5 (7)
S(2)–Sb(1)–S(4)	89.98 (4)	N(1)–C(2)–C(9)^c	111 (1)
S(3)–Sb(2)–S(4)	98.85 (4)	C(2)–N(1)–C(3)^c	130.1 (8)
S(4)–Sb(2)–S(4)^c	96.07 (5)	C(3)–N(1)–C(3)^c	110 (1)
Sb(1)–S(1)–Sb(1)^a	94.83 (5)	N(1)–C(1)–C(8)	134 (1)
Sb(1)–S(2)–Sb(1)^b	100.24 (6)	C(1)–C(8)–C(4)	112 (1)
Sb(1)–S(4)–Sb(2)	91.51 (3)	C(2)^c–C(9)–C(5)	112 (1)

Symmetry operation codes: $^a X, 2 - Y, 1 - Z$. $^b X, Y, {}^1/_2 - Z$. $^c X, Y, {}^3/_2 - Z$.

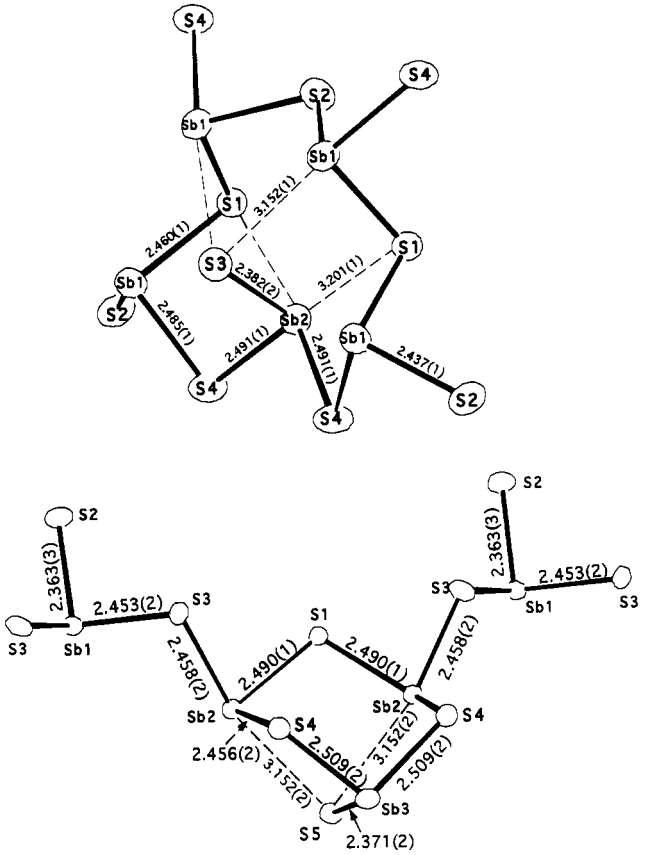

Figure 2. ORTEP drawing[24] of individual building units which constitute the 1-D chains found in (a, top) $Sb_3S_5{\cdot}N(C_3H_7)_4$ and (b, bottom) $Sb_4S_7{\cdot}N_2C_4H_8$. In the former material, edge-sharing five-membered rings, consisting of five corner-linked SbS_3-pyramids, link along the *a*-axial direction to form chains (Figure 1a). For (b) three-membered rings forming structures reminiscent of the semicube described previously[2] are linked by individual SbS_3 pyramids (Figure 1b). Selected interatomic distances are in angstroms and distances less than 2.5 Å are emphasized.

$[TPA]^+$ and $[N_2C_4H_8]^{2+}$ do not form three-dimensional systems of channels. Instead, the structures of SbStpa and SbSpip (Figure 1) consist of antimony sulfide pyramids which are linked to form chains of fused five- and three-membered rings respectively (Figure 2). These chains, infinite in the *a*-axial direction, are separated by the

Table VII. Selected Interatomic Distances (angstroms) and Angles (degrees) for SbSpip

Sb(1)–S(2)	2.363 (3)	C(1)–C(2)	1.508 (10)
Sb(1)–S(3)	2.453 (2)	S(1)···S(5)	3.824 (3)
Sb(2)–S(1)	2.490 (1)	Sb(2)···S(5)^c	3.152 (2)
Sb(2)–S(3)	2.458 (2)	Sb(2)···S(5)^e	3.244 (1)
Sb(2)–S(4)^b	2.456 (2)	S(1)···S(3)^c	3.283 (2)
Sb(3)–S(4)	2.509 (2)	S(1)···N(2)	3.236 (9)
Sb(3)–S(5)^d	2.371 (2)	S(2)···N(1)^g	3.108 (9)
N(1)–C(2)	1.493 (8)	S(2)···N(1)^f	3.148 (10)
N(2)–C(1)	1.510 (8)	S(4)···N(2)	3.360 (6)
S(2)–Sb(1)–S(3)	93.19 (6)	Sb(2)–S(1)–Sb(2)^c	110.28 (8)
S(3)–Sb(1)–S(3)^a	93.9 (1)	Sb(1)–S(3)–Sb(2)	102.04 (7)
S(1)–Sb(2)–S(3)	83.15 (6)	Sb(2)^d–S(4)–Sb(3)	98.37 (7)
S(1)–Sb(2)–S(4)^b	93.59 (7)	C(2)–N(1)–C(2)^c	110.3 (8)
S(3)–Sb(2)–S(4)^b	93.65 (7)	C(1)–N(2)–C(1)^c	111.0 (7)
S(4)–Sb(3)–S(4)^c	97.68 (8)	N(2)–C(1)–C(2)	110.8 (6)
S(4)–Sb(3)–S(5)^d	96.08 (6)	N(1)–C(2)–C(1)	110.2 (6)

Symmetry operation codes: $^a {}^3/_2 - X, Y, Z$. $^b X, Y, 1 + Z$. $^c {}^1/_2 - X, Y, Z$. $^d X, Y, -1 + Z$. $^e 1 - X, 1 - Y, Z$. $^f 1 - X, {}^3/_2 - Y, {}^1/_2 + Z$. $^g 1 - X, {}^3/_2 - Y, -{}^1/_2 + Z$.

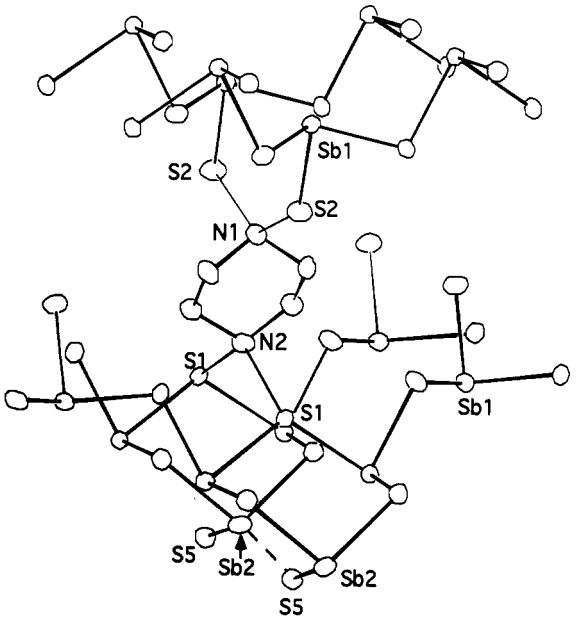

Figure 3. ORTEP drawing[24] of the environment about the $[N_2C_4H_8]^{2+}$ between the sheets formed by the chains of antimony sulfide in $Sb_3S_5{\cdot}N(C_3N_7)_4$. For the sake of clarity, only Sb–S distances <2.5 Å are shown. The short Sb–S contact (Table VII) between the individual chains, shown in Figure 2b, is represented as a dashed line.

$[TPA]^+$ or $[N_2C_4H_8]^{2+}$ ions (Figures 1–3). More detailed descriptions are given below.

SbStpa. The coordination geometry for Sb in this material is only approximately pyramidal. If Sb–S distances to 3.2 Å are included, Sb(2) is five- and Sb(1) four-coordinated to sulfur (Figure 2a). The $5s^2$ lone pairs associated with Sb^{3+} presumably occupy the space opposite the Sb(2)–S(3) bond and opposite the bisector of the S(2)–Sb(1)–S(1) bond angle (Figure 2). The geometry of five-membered rings (Figures 1 and 2) appears to be dictated by the bonding requirements of S(3). The $[TPA]^+$ cation separates the chains sufficiently that interchain bonding is not possible. Rather, to satisfy its bonding requirements, the S(3) atom is bent upward to bond intrachain with the Sb(1) atoms (Figure 2). It may be that $Sb_3S_5{\cdot}TPA$ could be a precursor for the synthesis of new materials if the five-membered rings are encouraged to unfold.

The individual chains of $[Sb_3S_5]^-$ are effectively isolated one from the other by the $[TPA]^+$ ions (Figure 1). The

closest Sb–S interchain distance is 7.1 Å, creating a 1-D antimony sulfide polymer. The light yellow color of this material contrasts with the deeper coloration of others in this family produced thus far[2,3] and for Sb_2S_3 itself; its density (Table III) is about 25% lower than for SbStma[3].

SbSpip. The local geometries found in SbSpip and SbStpa are compared in Figure 2. The coordination of antimony to sulfur to SbSpip is reminiscent of the "semicube" arrangement found in the 2-D antimony sulfide $Cs_6Sb_{10}S_{18}$.[2] In the case of the latter compound the "semicubes" are linked via SbS_3 pyramids to form rings. For SbSpip these semicubes are linked by similar pyramids to form chains.

Although the "chains" are emphasized in the drawings of this structure (Figures 1–3) the interchain distances are short enough that they can be considered to form slabs in (010). The distance between chains in the slab, emphasized in Figure 2, is 3.2 Å; this is shown as the Sb(5)–S(2) distance in Figure 3 and in Table VII. The organic molecule does not interleave with every antimony sulfide chain, as is the case for the TPA material. Instead, the piperazinium ion $[N_2C_4H_8]^{2+}$ alternates with the 2-D slabs of antimony sulfide and is hydrogen bonded to sulfurs in them as shown in Figure 3, where the N(1)···S distances are less than 3.2 Å (Table VII).

Conclusion

The family of novel open sulfides based upon Sb_2S_3 has been expanded. The synthetic techniques described here are quite general and, as was first demonstrated by Bedard and co-workers,[1] can be applied to a large variety of sulfide precursors to produce novel structure types.[2,3] The noncentrosymmetric space group symmetry was confirmed by the observation of a second harmonic signal, but their values, approximately 4 times that of quartz, exclude these compounds as viable second harmonic materials. However, new materials based upon the synthetic strategy outlined here may have more useful nonlinear optical properties.

Acknowledgment. We are grateful for the technical assistance of W. J. Marshall and D. Reardon for collection of X-ray and optical data. We are grateful for the efforts of Christopher Cahill for his assistance with the manuscript. This work is supported by National Science Foundation through grant DMR 9024249 and by the DuPont Company.

Supplementary Material Available: Tables of anisotropic thermal parameters for SbStpa and SbSpip (1 page); listing of structure factor amplitudes and anisotropic thermal parameters (14 pages). Ordering information is given on any current masthead page.

Additions and Corrections

1992, Volume 4.

Ren-Chain Wang, Yiping Zhang, Hengliang Hu, Roberto R. Frausto, and Abraham Clearfield*: Preparation of Lanthanide Arylphosphonates and Crystal Structures of Lanthanum Phenyl- and Benzylphosphonates.

Page 864. The following should be included at the end of the paper:

Supplementary Material Available: Listings of positional parameters, bond angles, bond distances and U values for $La(O_3PCH_2C_6H_5)(HO_3PCH_2C_6H_5)\cdot 2H_2O$ (10 pages); listings of structure factor amplitudes for $La(O_3PCH_2C_6H_5)(HO_3PCH_2C_6H_5)\cdot 2H_2O$ and $La(O_3PC_6H_5)(HO_3PC_6H_5)$ (26 pages). Ordering information is given on any current masthead page.